

First Lattice QCD determination of semileptonic decays of charmed-strange baryons

Ξ_c

Qi-An Zhang,¹ Jun Hua,² Fei Huang,² Renbo Li,³ Yuanyuan Li,³
Cai-Dian Lü,^{4,5} Peng Sun,^{3,*} Wei Sun,⁴ Wei Wang,^{2,†} and Yi-Bo Yang^{6,7,8,‡}

¹Key Laboratory for Particle Astrophysics and Cosmology (MOE),
Shanghai Key Laboratory for Particle Physics and Cosmology,

Tsung-Dao Lee Institute, Shanghai Jiao Tong University, Shanghai 200240, China

²INPAC, Key Laboratory for Particle Astrophysics and Cosmology (MOE),
Shanghai Key Laboratory for Particle Physics and Cosmology,

School of Physics and Astronomy, Shanghai Jiao Tong University, Shanghai 200240, China

³Nanjing Normal University, Nanjing, Jiangsu, 210023, China

⁴Institute of High Energy Physics, Chinese Academy of Sciences, Beijing 100049, China

⁵School of Physics, University of Chinese Academy of Sciences, Beijing 100049, China

⁶CAS Key Laboratory of Theoretical Physics, Institute of Theoretical Physics,
Chinese Academy of Sciences, Beijing 100190, China

⁷School of Fundamental Physics and Mathematical Sciences,

Hangzhou Institute for Advanced Study, UCAS, Hangzhou 310024, China

⁸International Centre for Theoretical Physics Asia-Pacific, Beijing/Hangzhou, China

(Dated: January 25, 2022)

While the standard model is the most successfully theory to describe all interactions and constituents in elementary particle physics, it has been constantly examined for over four decades. Weak decays of charm quarks can measure the coupling strength of quarks in different families and serve as an ideal probe for CP violation. As the lowest charm-strange baryons with three different flavors, Ξ_c baryons (made of csu or csd) have been extensively studied in experiments at the large hadron collider and in electron-positron collision. However the lack of reliable knowledge in theory becomes the unavoidable obstacle in the way. In this work, we use the state-of-the-art Lattice QCD techniques, and generate 2+1 clover fermion ensembles with two lattice spacings, $a = (0.108\text{fm}, 0.080\text{fm})$. We then present the first *ab-initio* lattice QCD determination of form factors governing $\Xi_c \rightarrow \Xi\ell^+\nu_\ell$, analogous with the notable β -decay of nuclei. Our theoretical results for decay widths are consistent with and about two times more precise than the latest measurements by ALICE and Belle collaborations. Together with experimental measurements, we independently determine the quark-mixing matrix element $|V_{cs}|$, which is found in good agreement with other determinations.

Introduction. Since the establishment in 1960s, the standard model (SM) of particle physics has achieved many remarkable successes, and has been constantly examined for over four decades. Nowadays searching for new physics (NP) beyond the SM is the primary objective in particle physics, which usually proceeds in two distinct directions. On the one side, new particles can be directly produced in high energy collisions for instance at the large hadron collider. On the other side, it is greatly valuable to examine various low-energy observables with prestigious high precision that can give an indirect search for NP.

Weak decays of heavy charm and bottom quarks provide an ideal platform to test the standard model of particle physics, especially the Cabibbo-Kobayashi-Maskawa (CKM) paradigm which describes quark mixing and CP violation. Any significant deviation from SM expectation for CKM matrix would indirectly provide definitive clues for new physics beyond SM. Most of previous analysis concentrated on the meson sector like B and D mesons, while recently heavy baryon decays started to determine $|V_{ub}/V_{cb}|$ from $\Lambda_b \rightarrow p\mu^-\bar{\nu}_\mu$ and $\Lambda_b \rightarrow \Lambda_c\mu^-\bar{\nu}_\mu$ [1], and $|V_{cs}|$ from $\Lambda_c \rightarrow \Lambda e^+\nu_e$ [2, 3].

The study of weak decays of charmed baryons $\Xi_c^{+,0}$ especially $\Xi_c \rightarrow \Xi\ell^+\nu$ decays is greatly valuable from various aspects. First of all, the combination of form factors from lattice QCD (LQCD) and experimental results for branching fractions of semileptonic decays allows an independent determination of $|V_{cs}|$. Secondly, a comparison of theory calculation and experimental measurements provides a stringent test of theoretical models. Thirdly, compared to the isosinglet counterpart Λ_c whose decays have been extensively in experiment [4–12] and from LQCD [13, 14], the iso-doublet $\Xi_c^{+,0}$ baryons have more versatile decay modes. The closeness of decay branching fractions for the exclusive $\Lambda_c \rightarrow \Lambda\ell^+\nu$ and inclusive $\Lambda_c \rightarrow X\ell^+\nu$ modes [8] shows a very different pattern with heavy bottom/charm mesons. The study of $\Xi_c \rightarrow \Xi\ell^+\nu$ decays and a combination with Λ_c decays can provide a way to validate this pattern, which is valuable to understand the underlying dynamics in baryonic transition, and test the flavor SU(3) symmetry [15–17]. Moreover, decays of Ξ_c have played an important role in the study of doubly-charmed baryon Ξ_{cc}^{++} [18], precision measurement of the lifetime of Ξ_b^0 [19] and the discovery of new exotic hadron candidates Ω_c [20].

Since the first observation of the inclusive semilep-

tonic decay [21], a number of different decay modes of Ξ_c have been studied in experiments [22–26]. In addition to measuring branching fractions for suppressed modes, the LHCb has also searched for CP violation in $\Xi_c^+ \rightarrow pK^-\pi^+$ [25]. Very recently, the ALICE [27] and Belle [28] collaborations have measured the branching fractions for $\Xi_c \rightarrow \Xi \ell^+ \nu$:

$$\mathcal{B}_{\text{ALICE}}(\Xi_c^0 \rightarrow \Xi^- e^+ \nu_e) = (2.43 \pm 0.25 \pm 0.35 \pm 0.72)\%, \quad (1)$$

$$\mathcal{B}_{\text{Belle}}(\Xi_c^0 \rightarrow \Xi^- e^+ \nu_e) = (1.72 \pm 0.10 \pm 0.12 \pm 0.50)\%, \quad (2)$$

$$\mathcal{B}_{\text{Belle}}(\Xi_c^0 \rightarrow \Xi^- \mu^+ \nu_\mu) = (1.71 \pm 0.17 \pm 0.13 \pm 0.50)\%, \quad (3)$$

where the last errors arise from the uncertainties in $\mathcal{B}(\Xi_c^0 \rightarrow \Xi^- \pi^+)$ [26].

On theoretical side, the $\Xi_c \rightarrow \Xi$ transition depends on six form factors which parametrize the matrix elements of vector and axial-vector currents between the Ξ_c and Ξ baryons. Most available theoretical analyses of these form factors are based on phenomenological models [29–34], but results vary substantially depending on explicit assumptions. A first-principle calculation is extremely crucial for a precise determination of CKM matrix element, and reliable analysis of CP violation in nonleptonic decays. In this work, we use the state-of-the-art LQCD techniques and for the first time in the literature calculate $\Xi_c \rightarrow \Xi$ form factors. Predictions for semi-leptonic decay widths are also presented, based on which the $|V_{cs}|$ is extracted. As we will show, our results greatly improve the theoretical calculations, and are more precise than the experimental measurements. These results also serve as mandatory inputs for future analysis of non-leptonic decays particularly in the factorization scheme.

Lattice Setup. This work is based on 2+1 flavor ensembles generated with tree level tadpole improved clover fermion action and tadpole improved Symanzik gauge action. One step of Stout link smearing is applied to the gauge field used by the clover action to improve the stability of the pion mass for given bare quark mass. The tadpole improvement factors for quarks and gluons are tuned to the fourth root of the plaquette using Stout link smearing and the original gauge links. We start from the ensemble s108 with bare coupling $\beta = \frac{10}{g^2} = 6.20$ and size $24^3 \times 72$, determine the lattice spacing using Wilson flow [35], and tune the bare coupling for the s080 ensemble with smaller lattice spacing to make their physical volume to be roughly the same. The information on the two ensembles used in this letter can be found in Tab. I.

TABLE I. Parameters of the 2+1 flavor clover fermion ensembles used in this calculation. The π/η_s masses and the lattice spacings are given in units of MeV, and fm, respectively.

	$\beta = \frac{10}{g^2}$	$L^3 \times T$	a	c_{sw}	κ_l	m_π	κ_s	m_{η_s}
s108	6.20	$24^3 \times 72$	0.108	1.161	0.1343	290	0.1330	640
s080	6.41	$32^3 \times 96$	0.080	1.141	0.1326	300	0.1318	650

On these two ensembles, we use the charm quark mass

$m_c^{s108} a = 0.485$ and $m_c^{s080} a = 0.235$, respectively, by requiring the corresponding J/ψ mass to have its physical value $m_{J/\psi} = 3.96900(6)\text{GeV}$ [36] within 0.3% accuracy.

The extraction of $\Xi_c \rightarrow \Xi$ form factors requires the lattice QCD calculation of both three-point correlation function (3pt) from Ξ_c to Ξ , and also the two point correlation functions (2pt) of both Ξ_c and Ξ . The 3pt with weak current $J^\mu = V^\mu - A^\mu = \bar{s}\gamma^\mu(1 - \gamma_5)c$ is defined by,

$$C_3^{V-A}(q^2, t, t_{\text{seq}}) = \int d^3\vec{x} d^3\vec{y} e^{-i\vec{p}_\Xi \cdot \vec{x}} e^{-i\vec{q} \cdot \vec{y}} T_{\gamma'\gamma} \times \langle 0 | \chi_\gamma^\Xi(\vec{x}, t_{\text{seq}}) J^\mu(\vec{y}, t) \bar{\chi}_{\gamma'}^{\Xi_c}(\vec{0}, 0) | 0 \rangle, \quad (4)$$

where χ_γ^{Ξ, Ξ_c} is the interpolation field of Ξ and Ξ_c , respectively, T is a combination of the Dirac matrix that is chosen to project out the form factor. For the 2pt with $B = \Xi, \Xi_c$,

$$C_2^B(t) = \int d^3\vec{x} e^{-i\vec{p}_B \cdot \vec{x}} T_{\gamma'\gamma} \langle 0 | \chi_\gamma^B(\vec{x}, t) \bar{\chi}_{\gamma'}^B(\vec{0}, 0) | 0 \rangle, \quad (5)$$

we choose T' as the identity matrix to simplify the expressions. Then we can define the following ratios for different projection matrices T and current operator V^μ/A^μ ,

$$R_{V/A}(T, \mu) = \sqrt{\frac{C_3^{V/A}(q^2, t, t_{\text{seq}}) C_3^{V/A}(q^2, t_{\text{seq}} - t, t_{\text{seq}})}{C_2^{B_1}(t_{\text{seq}}) C_2^{B_2}(t_{\text{seq}})}}, \quad (6)$$

where the subscript V or A corresponds to the vector or axial-vector current in the 3pt. After making use of the reduction formula, the ratios R_F for the six form factors $F = (f_\perp, f_+, f_0, g_\perp, g_+, g_0)$ can be constructed by different combinations of $R_{V/A}(T, \mu)$. More details can be found in the supplemental material [37]. Then we adopt the parameterization,

$$R_F = F \left(\frac{1 + c_1 e^{-\Delta E_1 t} + c_2 e^{-\Delta E_2 (t_{\text{seq}} - t)}}{1 + d_1 e^{-\Delta E_1 t_{\text{seq}}}} \frac{1 + c_1 e^{-\Delta E_1 (t_{\text{seq}} - t)} + c_2 e^{-\Delta E_2 t}}{1 + d_2 e^{-\Delta E_2 t_{\text{seq}}}} \right)^{1/2} \quad (7)$$

$$\simeq F [1 + c'_1 (e^{-\Delta E_1 t/2} + e^{-\Delta E_1 (t_{\text{seq}} - t)}) / 2], \quad (8)$$

to eliminate excited-state contaminations and obtain the desired form factor F , where ΔE_1 and ΔE_2 ($> \Delta E_1$) describe the mass differences between the first excited states and ground states in the initial and final interpolation fields. It should be noted that Eq. (7) is employed in the fit for most cases, while Eq. (8) is used for large negative q^2 in combination with the ensemble s080 since the lattice results are noisy. We have checked that in these cases using Eq. (7) will lead to consistent central values.

The vector and axial-vector $c \rightarrow s$ currents on the lattice suffer from finite renormalization. Such a renormalization can be defined by the ratio of the conserved-vector-current-like V_c and the local current V in the

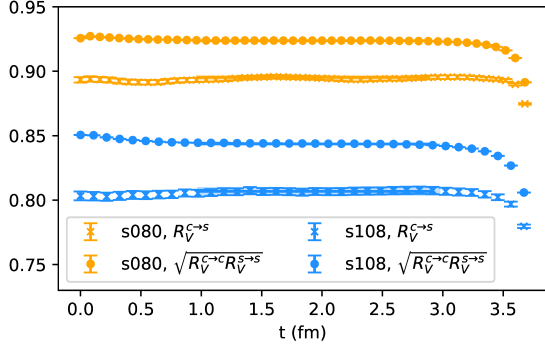


FIG. 1. Lattice results for $R_V^{c \rightarrow s}$ and $\sqrt{R_V^{c \rightarrow c} R_V^{s \rightarrow s}}$. The bands correspond to the ground state contributions $Z_V^{c \rightarrow s}$ and $\sqrt{Z_V^{c \rightarrow c} Z_V^{s \rightarrow s}}$ on the s080 and s108 ensembles, respectively.

hadron matrix element,

$$\begin{aligned} R_V^{q_1 \rightarrow q_2}(t) &= \frac{\langle M_1(T/2) \sum_{\vec{x}} V_c^{q_1 \rightarrow q_2}(\vec{x}, t) M_2(0) \rangle}{\langle M_1(T/2) \sum_{\vec{x}} V^{q_1 \rightarrow q_2}(\vec{x}, t) M_2(0) \rangle} \\ &= Z_V^{q_1 \rightarrow q_2} + \mathcal{O}(e^{-T/4\Delta E}), \end{aligned} \quad (9)$$

where $M_{1,2}$ are arbitrary pseudoscalar states and ΔE is the mass gap between the ground state and first excited state. For the $c \rightarrow s$ current, one can use either the combination $(M_1, M_2) = (\eta_s, D_s)$, or the geometric average of those of the $s \rightarrow s$ current and $c \rightarrow c$ current using $(M_1, M_2) = (\eta_s, \eta_s)$ and (η_c, η_c) , respectively. We illustrate the Z_V in Fig. 1, in which the crosses and dots correspond to $R_V^{c \rightarrow s}(t)$ and $\sqrt{R_V^{c \rightarrow c}(t) R_V^{s \rightarrow s}(t)}$, respectively. Constant fits can describe the data at medium large $t \sim T/4$ well, and the difference between two definitions becomes smaller for the finer s080 ensemble (upper yellow data), and both of them are also closer to one compared to the values for the coarser s108 ensemble (lower blue data). Thus the differences between the two strategies arise from discretization effects. In the following discussion, we will use $Z_V^{c \rightarrow s}$ to obtain the central values of the final result, then repeat the analysis with $\sqrt{Z_V^{c \rightarrow c} Z_V^{s \rightarrow s}}$ and treat the differences as a systematic uncertainty. Due to the chiral symmetry breaking of the clover fermion action, the renormalization factor of the axial-vector current is not exactly the same as for the vector one. Thus we use the off-shell quark matrix elements to define Z_A as,

$$Z_A^{c \rightarrow s} \equiv Z_V^{c \rightarrow s} \sqrt{\frac{\text{Tr}[\langle c | V^\mu | c \rangle \gamma^\mu \gamma_5] \text{Tr}[\langle s | V^\mu | s \rangle \gamma^\mu \gamma_5]}{\text{Tr}[\langle c | A^\mu | c \rangle \gamma^\mu] \text{Tr}[\langle s | A^\mu | s \rangle \gamma^\mu]}}, \quad (10)$$

with multiple off-shell quark momenta p^2 . With $a^2 p^2$ extrapolation using three values of p^2 in the range of $a^2 p^2 \in [4, 8]$, we obtained $Z_A/Z_V = 1.010231(69)$ and $1.020296(68)$ on s108 and s080, respectively.

Numerical Results. By choosing different reference time slices, we perform 48×393 measurements on the s108 ensemble, and 72×436 measurements on the s080 ensemble. The lattice results for the ratios R_{f_\perp} with $\vec{p}_\Xi = (0, 0, 1) \times \frac{2\pi}{L_a} (\frac{2\pi}{L_a} \simeq 0.48 \text{ GeV})$ are shown in Fig. 2. The $\chi^2/d.o.f$ are below/close to 1 for most fits of 400 bootstrap samples, which indicates a good fit quantity, and the colored bands in the left panel of Fig. 2 predicted by the fit agree with the data points well. To further validate the results, we calculate the differential summed ratio [38],

$$\tilde{R}(t_{\text{seq}}) \equiv \frac{SR(t_{\text{seq}}) - SR(t_{\text{seq}} - \Delta t)}{\Delta t}, \quad (11)$$

and show the results in the right panel of Fig. 2, where $SR(t_{\text{seq}}) \equiv \sum_{t_c < t < t_{\text{seq}} - t_c} R_F(t, t_{\text{seq}})$, $t_c = 3a$ is the requirement used in the fits to suppress higher excited states contributions. One can see that $\tilde{R}(t_{\text{seq}})$ agrees with the grey band from the two-state fit well when $t_{\text{seq}} > 14a$.

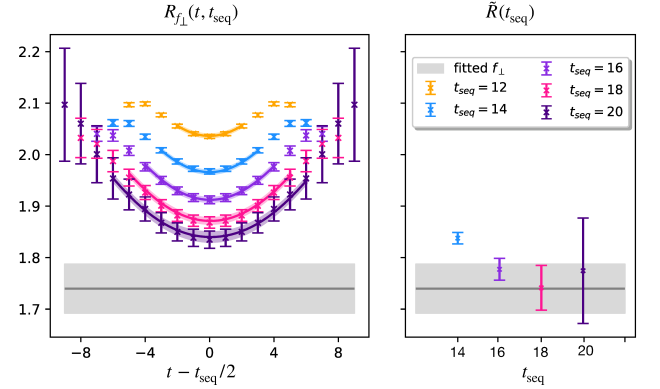


FIG. 2. Lattice results for the $f_\perp(\Xi_c \rightarrow \Xi)$ form factor on the s080 ensemble with $\vec{p}_\Xi = (0, 0, 1) \times \frac{2\pi}{L_a}$, in the source-sink separation range $[12a, 20a]$. The left panel shows a two-state fit with the excited state contamination using the parametrization defined in Eq. (7), and the right panel gives the differential summed ratio. The ground-state matrix element (the grey band) obtained from the two-state fit agree with the differential summed ratio well when $t_{\text{seq}} > 14$.

To access the q^2 distribution, we employ the z -expansion parametrization of form factors that arises from analyticity and unitarity [39]

$$f(q^2) = \frac{1}{1 - q^2/(m_{\text{pole}}^f)^2} \sum_{n=0}^{n_{\text{max}}} (c_n^f + d_n^f a^2) [z(q^2)]^n, \quad (12)$$

where

$$z(q^2) = \frac{\sqrt{t_+ - q^2} - \sqrt{t_+ - t_0}}{\sqrt{t_+ - q^2} + \sqrt{t_+ - t_0}}. \quad (13)$$

$t_0 = q_{\text{max}}^2 = (m_{\Xi_c} - m_\Xi)^2$ and $t_+ = (m_D + m_K)^2$, and d_n^f describes the discretization error of each z -expansion

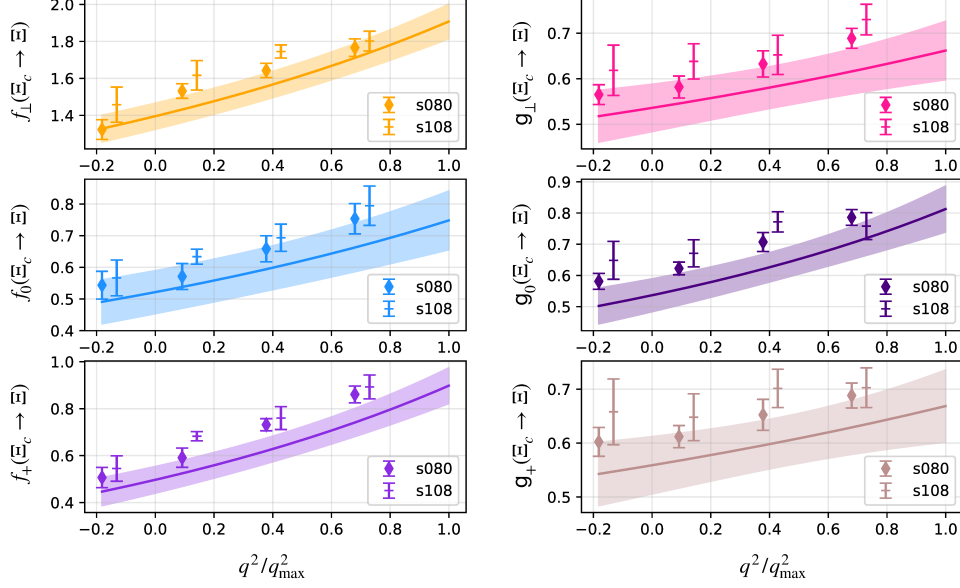


FIG. 3. The q^2 distribution for the $\Xi_c \rightarrow \Xi$ form factors. The z expansion approach has been used to fit the lattice data. An extrapolation to the continuum limit has been made, and the shaded regions correspond to the final results with $a \rightarrow 0$.

parameter c_n^f . The pole masses in the form factor are $m_{\text{pole}}^{f_+, f_\perp} = 2.112$ GeV, $m_{\text{pole}}^{f_0} = 2.318$ GeV, $m_{\text{pole}}^{g_+, g_\perp} = 2.460$ GeV, and $m_{\text{pole}}^{g_0} = 1.968$ GeV. We collect the fitted parameters in Tab. II, and show the q^2 dependent form factor in the continuum limit (by eliminating the d_n^f terms) from the fit and also the Lattice results at given q^2 in Fig. 3. As shown in the figure, our form factor results for the s108 ensemble and the s080 ensemble show only small discretization effects.

TABLE II. Results for the z -expansion parameters describing the form factors with statistical errors.

	c_0	c_1	c_2
f_\perp	1.51 ± 0.09	-1.88 ± 1.21	1.71 ± 0.49
f_0	0.64 ± 0.09	-1.83 ± 1.22	0.56 ± 0.51
f_+	0.77 ± 0.07	-4.09 ± 1.18	0.35 ± 0.49
g_\perp	0.56 ± 0.07	-0.35 ± 1.26	0.15 ± 0.29
g_0	0.63 ± 0.07	-1.37 ± 1.36	0.15 ± 0.29
g_+	0.56 ± 0.08	0.00 ± 1.38	0.14 ± 0.29

In Fig. 4, we use the above form factors to predict differential decay widths (in units of $\text{ps}^{-1}\text{GeV}^{-2}$) for $\Xi_c^0 \rightarrow \Xi^- \ell^+ \nu$ divided by $|V_{cs}|^2$ as a function of q^2 . Results for $\Xi_c^+ \rightarrow \Xi^0 \ell^+ \nu$ are also similar. Using the lifetime from PDG: $\tau(\Xi_c^0) = (1.53 \pm 0.06) \times 10^{-13}\text{s}$ and $\tau(\Xi_c^-) = (4.56 \pm 0.05) \times 10^{-13}\text{s}$, and $|V_{cs}| = 0.97320 \pm 0.00011$ [36],

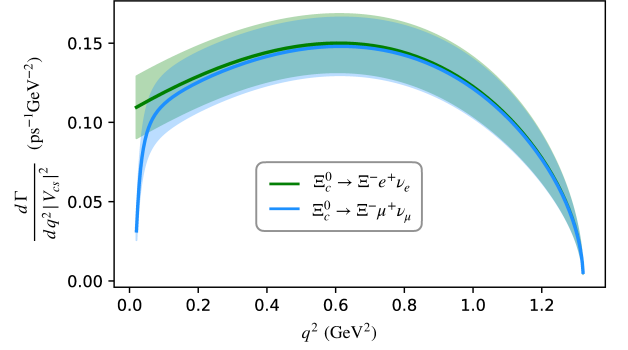


FIG. 4. Predictions for the differential decay widths for the $\Xi_c^0 \rightarrow \Xi^- e^+ \nu_e$ and $\Xi_c^0 \rightarrow \Xi^- \mu^+ \nu_\mu$, divided by $|V_{cs}|^2$ in units of $\text{ps}^{-1}\text{GeV}^{-2}$.

one can obtain the decay branching fractions:

$$\begin{aligned}
 \mathcal{B}(\Xi_c^0 \rightarrow \Xi^- e^+ \nu_e) &= 2.38(0.30)_{\text{stat.}}(0.32)_{\text{ext.}}(0.07)_{\text{ren.}}\%, \\
 \mathcal{B}(\Xi_c^0 \rightarrow \Xi^- \mu^+ \nu_\mu) &= 2.29(0.29)_{\text{stat.}}(0.30)_{\text{ext.}}(0.06)_{\text{ren.}}\%, \\
 \mathcal{B}(\Xi_c^+ \rightarrow \Xi^0 e^+ \nu_e) &= 7.18(0.90)_{\text{stat.}}(0.96)_{\text{ext.}}(0.20)_{\text{ren.}}\%, \\
 \mathcal{B}(\Xi_c^+ \rightarrow \Xi^0 \mu^+ \nu_\mu) &= 6.91(0.87)_{\text{stat.}}(0.91)_{\text{ext.}}(0.19)_{\text{ren.}}\%.
 \end{aligned} \tag{14}$$

The first errors come from statistical fluctuations, while the second and third ones are systematic uncertainties arising from the differences between continuum-

extrapolated results and the ones using the s080 ensemble, and the differences between the results using $Z_{V/A}^{c \rightarrow s}$ or $\sqrt{Z_{V/A}^{c \rightarrow c} Z_{V/A}^{s \rightarrow s}}$ in the renormalization, respectively. Our predictions for branching fractions are consistent with model predictions in Ref. [29], but smaller than the ones in Ref. [30, 33]. Compared to the previous theoretical results which have typically 30% ~ 50% parametric uncertainties and uncontrollable systematic uncertainties, our results have greatly improved the theoretical predictions. Our calculation also indicates sizable SU(3) symmetry breaking effects compared to $\Lambda_c \rightarrow \Lambda \ell^+ \nu$ decays [3, 13].

The ratio of branching fractions is predicted as:

$$R_{\mu/e} = \frac{\mathcal{B}(\Xi_c^0 \rightarrow \Xi^- \mu^+ \nu_\mu)}{\mathcal{B}(\Xi_c^0 \rightarrow \Xi^- e^+ \nu_e)} = \frac{\mathcal{B}(\Xi_c^+ \rightarrow \Xi^0 \mu^+ \nu_\mu)}{\mathcal{B}(\Xi_c^+ \rightarrow \Xi^0 e^+ \nu_e)} = 0.962(0.003)_{\text{stat.}}(0.002)_{\text{syst.}}, \quad (15)$$

where most uncertainties from form factors have cancelled to a large extent. The deviation from unity arises from the mass differences between muon and electron. This result is consistent with and much more precise than the Belle measurement: $R_{\mu/e} = 1.00 \pm 0.11 \pm 0.09$ [28], which indicates that effects not covered by our lattice calculation are probably less significant at our level of precision.

Our results for branching fractions are consistent with and about two times more precise than the measurements by ALICE and Belle collaborations as shown in Eq. (1-3). Using the ALICE measurement [27], we give a determination of $|V_{cs}|$:

$$|V_{cs}| = 0.983(0.060)_{\text{stat.}}(0.065)_{\text{syst.}}(0.167)_{\text{exp.}}, \quad (16)$$

where the first two uncertainties are statistical and systematic uncertainties of the theoretical results, and the last ones are dominant and come from experimental data. Using the Belle result [28], we also have:

$$|V_{cs}| = 0.834(0.051)_{\text{stat.}}(0.056)_{\text{syst.}}(0.127)_{\text{exp.}}, \quad (17)$$

which is obtained by combing $\Xi_c^0 \rightarrow \Xi^- e^+ \nu_e$ and $\Xi_c^0 \rightarrow \Xi^- \mu^+ \nu_\mu$. Using the individual channel, we have $|V_{cs}|_{(\ell=e)} = 0.830(0.051)_{\text{stat.}}(0.055)_{\text{syst.}}(0.128)_{\text{exp.}}$ and $|V_{cs}|_{(\ell=\mu)} = 0.846(0.052)_{\text{stat.}}(0.056)_{\text{syst.}}(0.135)_{\text{exp.}}$. Both results of $|V_{cs}|$ from ALICE and Belle data are consistent with the global fit [36] within $1-\sigma$.

It is necessary to point out that the largest errors in the extracted results for $|V_{cs}|$ are from experimental data on $\mathcal{B}(\Xi_c^0 \rightarrow \Xi^- \pi^+)$ [26]. This can be improved by more precise measurements at LHCb, Belle-II, BESIII and other experiments in future. It should also be noted that as a conservative estimate, we have included systematic uncertainties (about 6%). In the continuum extrapolation, the statistical uncertainties in the two lattice ensembles are added and the final uncertainties are also about 6%.

Conclusions. We have reported the first lattice QCD calculation of the form factors governing the $\Xi_c \rightarrow \Xi \ell^+ \nu_\ell$

at two lattice spacings and extrapolated them to the continuum. Using the CKM matrix element $|V_{cs}|$ from PDG and the Ξ_c lifetimes, we predict the branching fractions $\mathcal{B}(\Xi_c^0 \rightarrow \Xi^- e^+ \nu_e) = 2.38(0.30)_{\text{stat.}}(0.32)_{\text{syst.}}\%$, $\mathcal{B}(\Xi_c^0 \rightarrow \Xi^- \mu^+ \nu_\mu) = 2.29(0.29)_{\text{stat.}}(0.31)_{\text{syst.}}\%$, $\mathcal{B}(\Xi_c^+ \rightarrow \Xi^0 e^+ \nu_e) = 7.18(0.90)_{\text{stat.}}(0.98)_{\text{syst.}}\%$, and $\mathcal{B}(\Xi_c^+ \rightarrow \Xi^0 \mu^+ \nu_\mu) = 6.91(0.87)_{\text{stat.}}(0.93)_{\text{syst.}}\%$ with both statistical and systematic uncertainties. Our results have greatly improved previous theoretical calculations, and are consistent with and about two times more precise than the measurements by ALICE and Belle collaborations. Our calculation also indicates sizable SU(3) symmetry breaking effects compared to $\Lambda_c \rightarrow \Lambda \ell^+ \nu$ decays. These results also serve as mandatory inputs for the analysis of non-leptonic decays in the factorization scheme. Using the measured branching fraction from two experiments together with our lattice results, we determine the CKM matrix element $|V_{cs}| = 0.983(0.060)_{\text{stat.}}(0.065)_{\text{syst.}}(0.167)_{\text{exp.}}$ and $0.834(0.051)_{\text{stat.}}(0.056)_{\text{syst.}}(0.127)_{\text{exp.}}$, where the errors come from the theoretical and experimental uncertainties, respectively.

Acknowledgment.— We thank Andreas Schäfer for valuable discussions, Y.B. Yin, J. Zhu and T. Cheng for pointing out the ALICE result in Ref. [27], C.P. Shen and Y.B. Li for the correspondence on the Belle measurement [28], and W.B. Qian, Y.H. Xie, H.B. Li, B.Q. Ke and X.R. Lyu for noticing us the experimental studies of Ξ_c decays at LHCb and BESIII. We greatly thank Prof. En-Ke Wang, Nu Xu and Rong-Gen Cai for their support when the gauge configurations are generated on the cluster supported by Southern Nuclear Science Computing Center (SNSC) and also HPC Cluster of ITP-CAS. The LQCD calculations were performed using the Chroma software suite [40] and QUDA [41–43] through HIP programming model [44]. The numerical calculation is supported by Chinese Academy of Science CAS Strategic Priority Research Program of Chinese Academy of Sciences, Grant No. XDC01040100. The setup for numerical simulations was conducted on the π 2.0 cluster supported by the Center for High Performance Computing at Shanghai Jiao Tong University. This work is supported in part by Natural Science Foundation of China under grant Nos. 11735010, U2032102, 11653003, 12005130, 11521505, 12070131001, 11975127 and 11935017, Natural Science Foundation of Shanghai under grant No. 15DZ2272100, the China Postdoctoral Science Foundation and the National Postdoctoral Program for Innovative Talents (Grant No. BX20190207), National Key Research and Development Program of China under Contract No. 2020YFA0406400, Jiangsu Specially Appointed Professor Program, the Strategic Priority Research Program of Chinese Academy of Sciences, Grant No. XDB34030300, and a NSFC-DFG joint

grant under grant No. 12061131006 and SCHA 458/22.

-
- * Corresponding author: sunpeng@njnu.edu.cn
† Corresponding author: wei.wang@sjtu.edu.cn
‡ Corresponding author: ybyang@itp.ac.cn
- [1] R. Aaij *et al.* [LHCb], *Nature Phys.* **11**, 743-747 (2015), doi:10.1038/nphys3415 [arXiv:1504.01568 [hep-ex]].
- [2] J. W. Hinson *et al.* [CLEO], *Phys. Rev. Lett.* **94**, 191801 (2005), doi:10.1103/PhysRevLett.94.191801 [arXiv:hep-ex/0501002 [hep-ex]].
- [3] M. Ablikim *et al.* [BESIII], *Phys. Rev. Lett.* **115**, 221805 (2015), doi:10.1103/PhysRevLett.115.221805 [arXiv:1510.02610 [hep-ex]].
- [4] M. Ablikim *et al.* [BESIII], *Phys. Rev. Lett.* **116**, 052001 (2016), doi:10.1103/PhysRevLett.116.052001 [arXiv:1511.08380 [hep-ex]].
- [5] M. Ablikim *et al.* [BESIII], *Phys. Rev. Lett.* **117**, 232002 (2016), doi:10.1103/PhysRevLett.117.232002 [arXiv:1608.00407 [hep-ex]].
- [6] M. Ablikim *et al.* [BESIII], *Phys. Rev. Lett.* **118**, 112001 (2017), doi:10.1103/PhysRevLett.118.112001 [arXiv:1611.02797 [hep-ex]].
- [7] M. Ablikim *et al.* [BESIII], *Phys. Lett. B* **772**, 388-393 (2017), doi:10.1016/j.physletb.2017.06.065 [arXiv:1705.11109 [hep-ex]].
- [8] M. Ablikim *et al.* [BESIII], *Phys. Rev. Lett.* **121**, no.25, 251801 (2018) doi:10.1103/PhysRevLett.121.251801 [arXiv:1805.09060 [hep-ex]].
- [9] M. Ablikim *et al.* [BESIII], *Phys. Rev. D* **100**, no.7, 072004 (2019), doi:10.1103/PhysRevD.100.072004 [arXiv:1905.04707 [hep-ex]].
- [10] M. Ablikim *et al.* [BESIII], *Chin. Phys. C* **44**, 040001 (2020), doi:10.1088/1674-1137/44/4/040001 [arXiv:1912.05983 [hep-ex]].
- [11] A. Zupanc *et al.* [Belle], *Phys. Rev. Lett.* **113**, 042002 (2014), doi:10.1103/PhysRevLett.113.042002 [arXiv:1312.7826 [hep-ex]].
- [12] S. B. Yang *et al.* [Belle], *Phys. Rev. Lett.* **117**, 011801 (2016), doi:10.1103/PhysRevLett.117.011801 [arXiv:1512.07366 [hep-ex]].
- [13] S. Meinel, *Phys. Rev. Lett.* **118**, 082001 (2017), doi:10.1103/PhysRevLett.118.082001 [arXiv:1611.09696 [hep-lat]].
- [14] S. Meinel, *Phys. Rev. D* **97**, 034511 (2018), doi:10.1103/PhysRevD.97.034511 [arXiv:1712.05783 [hep-lat]].
- [15] C. D. Lü, W. Wang and F. S. Yu, *Phys. Rev. D* **93**, no.5, 056008 (2016) doi:10.1103/PhysRevD.93.056008 [arXiv:1601.04241 [hep-ph]].
- [16] Y. Grossman and S. Schacht, *Phys. Rev. D* **99**, no.3, 033005 (2019) doi:10.1103/PhysRevD.99.033005 [arXiv:1811.11188 [hep-ph]].
- [17] C. Q. Geng, C. W. Liu, T. H. Tsai and S. W. Yeh, *Phys. Lett. B* **792**, 214-218 (2019) doi:10.1016/j.physletb.2019.03.056 [arXiv:1901.05610 [hep-ph]].
- [18] R. Aaij *et al.* [LHCb], *Phys. Rev. Lett.* **121**, no.5, 052002 (2018) doi:10.1103/PhysRevLett.121.052002 [arXiv:1806.02744 [hep-ex]].
- [19] R. Aaij *et al.* [LHCb], *Phys. Rev. Lett.* **113**, 032001 (2014) doi:10.1103/PhysRevLett.113.032001 [arXiv:1405.7223 [hep-ex]].
- [20] R. Aaij *et al.* [LHCb], *Phys. Rev. Lett.* **118**, no.18, 182001 (2017) doi:10.1103/PhysRevLett.118.182001 [arXiv:1703.04639 [hep-ex]].
- [21] J. P. Alexander *et al.* [CLEO], *Phys. Rev. Lett.* **74**, 3113-3117 (1995) [erratum: *Phys. Rev. Lett.* **75**, 4155 (1995)], doi:10.1103/PhysRevLett.74.3113
- [22] R. Aaij *et al.* [LHCb], *JHEP* **04**, 084 (2019) doi:10.1007/JHEP04(2019)084 [arXiv:1901.06222 [hep-ex]].
- [23] R. Aaij *et al.* [LHCb], *Phys. Rev. D* **100**, no.3, 032001 (2019) doi:10.1103/PhysRevD.100.032001 [arXiv:1906.08350 [hep-ex]].
- [24] R. Aaij *et al.* [LHCb], *Phys. Rev. D* **102**, no.7, 071101 (2020) doi:10.1103/PhysRevD.102.071101 [arXiv:2007.12096 [hep-ex]].
- [25] R. Aaij *et al.* [LHCb], *Eur. Phys. J. C* **80**, no.10, 986 (2020) doi:10.1140/epjc/s10052-020-8365-0 [arXiv:2006.03145 [hep-ex]].
- [26] Y. B. Li *et al.* [Belle], *Phys. Rev. Lett.* **122**, 082001 (2019), doi:10.1103/PhysRevLett.122.082001 [arXiv:1811.09738 [hep-ex]].
- [27] J. Zhu on behalf of the ALICE collaboration, *PoS ICHEP2020* (2021) 524.
- [28] Y. B. Li *et al.* [Belle], [arXiv:2103.06496 [hep-ex]].
- [29] Z. X. Zhao, *Chin. Phys. C* **42**, 093101 (2018), doi:10.1088/1674-1137/42/9/093101 [arXiv:1803.02292 [hep-ph]].
- [30] Y. L. Liu and M. Q. Huang, *J. Phys. G* **37**, 115010 (2010), doi:10.1088/0954-3899/37/11/115010 [arXiv:1102.4245 [hep-ph]].
- [31] K. Azizi, Y. Sarac and H. Sundu, *Eur. Phys. J. A* **48**, 2 (2012), doi:10.1140/epja/i2012-12002-1 [arXiv:1107.5925 [hep-ph]].
- [32] C. Q. Geng, Y. K. Hsiao, C. W. Liu and T. H. Tsai, *Phys. Rev. D* **97**, no.7, 073006 (2018), doi:10.1103/PhysRevD.97.073006 [arXiv:1801.03276 [hep-ph]].
- [33] C. Q. Geng, C. W. Liu and T. H. Tsai, [arXiv:2012.04147 [hep-ph]].
- [34] Z. X. Zhao, [arXiv:2103.09436 [hep-ph]].
- [35] S. Borsanyi, S. Dürr, Z. Fodor, C. Hoelbling, S. D. Katz, S. Krieg, T. Kurth, L. Lellouch, T. Lipert and C. McNeile, *et al.* *JHEP* **09**, 010 (2012), doi:10.1007/JHEP09(2012)010 [arXiv:1203.4469 [hep-lat]].
- [36] P. A. Zyla *et al.* [Particle Data Group], *PTEP* **2020**, 083C01 (2020), doi:10.1093/ptep/ptaa104
- [37] Supplementary material of this work.
- [38] C. C. Chang, A. N. Nicholson, E. Rinaldi, E. Berkowitz, N. Garron, D. A. Brantley, H. Monge-Camacho, C. J. Monahan, C. Bouchard and M. A. Clark, *et al.* *Nature* **558**, 91-94 (2018), doi:10.1038/s41586-018-0161-8 [arXiv:1805.12130 [hep-lat]].
- [39] C. Bourrely, I. Caprini and L. Lellouch, *Phys. Rev. D* **79**, 013008 (2009) [erratum: *Phys. Rev. D* **82**, 099902 (2010)], doi:10.1103/PhysRevD.82.099902 [arXiv:0807.2722 [hep-ph]].
- [40] R. G. Edwards *et al.* [SciDAC, LHPC and UKQCD], *Nucl. Phys. B Proc. Suppl.* **140**, 832 (2005), doi:10.1016/j.nuclphysbps.2004.11.254 [arXiv:hep-lat/0409003 [hep-lat]].
- [41] M. A. Clark, R. Babich, K. Barros, R. C. Brower and

- C. Rebbi, *Comput. Phys. Commun.* **181**, 1517-1528 (2010), doi:10.1016/j.cpc.2010.05.002 [arXiv:0911.3191 [hep-lat]].
- [42] R. Babich, M. A. Clark, B. Joo, G. Shi, R. C. Brower and S. Gottlieb, doi:10.1145/2063384.2063478 [arXiv:1109.2935 [hep-lat]].
- [43] M. A. Clark, B. Joó, A. Strelchenko, M. Cheng, A. Gambhir and R. Brower, [arXiv:1612.07873 [hep-lat]].
- [44] Y. J. Bi, Y. Xiao, W. Y. Guo, M. Gong, P. Sun, S. Xu and Y. B. Yang, *PoS LATTICE2019*, 286 (2020), doi:10.22323/1.363.0286 [arXiv:2001.05706 [hep-lat]].